



OPEN ACCESS

EDITED BY

James Friend,
University of California, San Diego,
United States

REVIEWED BY

John Sharer Allen,
University of Hawaii at Manoa, United States
Athanasios Athanassiadis,
Heidelberg University, Germany

*CORRESPONDENCE

Ofer Manor,
✉ manoro@technion.ac.il

RECEIVED 28 January 2025

ACCEPTED 10 April 2025

PUBLISHED 05 June 2025

CITATION

Aremanda S, Li Y, Onuh G and Manor O (2025)
Measurement of dynamic electrokinetic effects
at the glass/electrolyte interface using a mega-
Hertz-level mechanical wave.
Front. Acoust. 3:1568083.
doi: 10.3389/facou.2025.1568083

COPYRIGHT

© 2025 Aremanda, Li, Onuh and Manor. This is
an open-access article distributed under the
terms of the [Creative Commons Attribution
License \(CC BY\)](#). The use, distribution or
reproduction in other forums is permitted,
provided the original author(s) and the
copyright owner(s) are credited and that the
original publication in this journal is cited, in
accordance with accepted academic practice.
No use, distribution or reproduction is
permitted which does not comply with these
terms.

Measurement of dynamic electrokinetic effects at the glass/electrolyte interface using a mega-Hertz-level mechanical wave

Sudeepthi Aremanda, Yifan Li, Gideon Onuh and Ofer Manor*

Department of Chemical Engineering, Technion – Israel Institute of Technology, Haifa, Israel

We measured the dynamic electrical properties of a spontaneously charged glass surface in an electrolyte solution by using a MHz-level surface acoustic wave (SAW) actuator to introduce a same-frequency mechanical wave into the glass substrate. The mechanical wave vibrated ions in the nanometer-thick electrical double layer (EDL) to appear at the glass/electrolyte interface. The out-of-equilibrium EDL leaked an electrical field, which was modulated by ion vibration frequency to reveal the presence of ions and their dynamic motion. A previous study excited EDLs on the piezoelectric lithium niobate substrate of a SAW actuator in contact with an electrolyte solution, but it remained unclear whether the mechanical or electrical components of the SAW in the piezoelectric substrate dominated the EDL excitation. Here, we isolated the SAW mechanical component in glass and showed that it introduces a similar ion electrokinetic vibration in the excited EDL at the glass/electrolyte interface using sodium nitrate and potassium chloride solutions as electrolytes. The measured electrical field leakage spectra were of similar magnitude to those measured in the previous study and exhibited similar non-monotonic behaviors, taking local maxima where the SAW period (the inverse of its frequency) was synchronized with the ion relaxation times in the EDL. At these frequencies, the synchronization maximized ion vibration displacement, thereby amplifying the electrical field leakage. Our findings may be used to study the electrokinetic properties of solid surfaces and ion dynamics in EDLs. Moreover, SAW-actuated fluidic platforms may support out-of-equilibrium EDLs relevant to ion-selective membranes and the film stability of electrolyte solutions.

KEYWORDS

surface acoustic wave, acoustic streaming, electroacoustics, electrokinetics, electrical double layer, electrolytes, relaxation time, bulk acoustic wave

1 Introduction

A MHz-level Rayleigh-type surface acoustic wave (SAW), traveling near the surface of a solid substrate, supports an accompanying sub-micrometer-thick evanescent mechanical wave (i.e., a spatiotemporal periodic boundary layer flow) in the neighboring water phase, whether the SAW is a standing wave (Rayleigh, 1884; Schlichting, 1932) or a traveling wave (Vanneste and Bühler, 2011; Manor et al., 2012). In a piezoelectric substrate, commonly used for SAW actuators, the SAW mechanical component is accompanied by a voltage

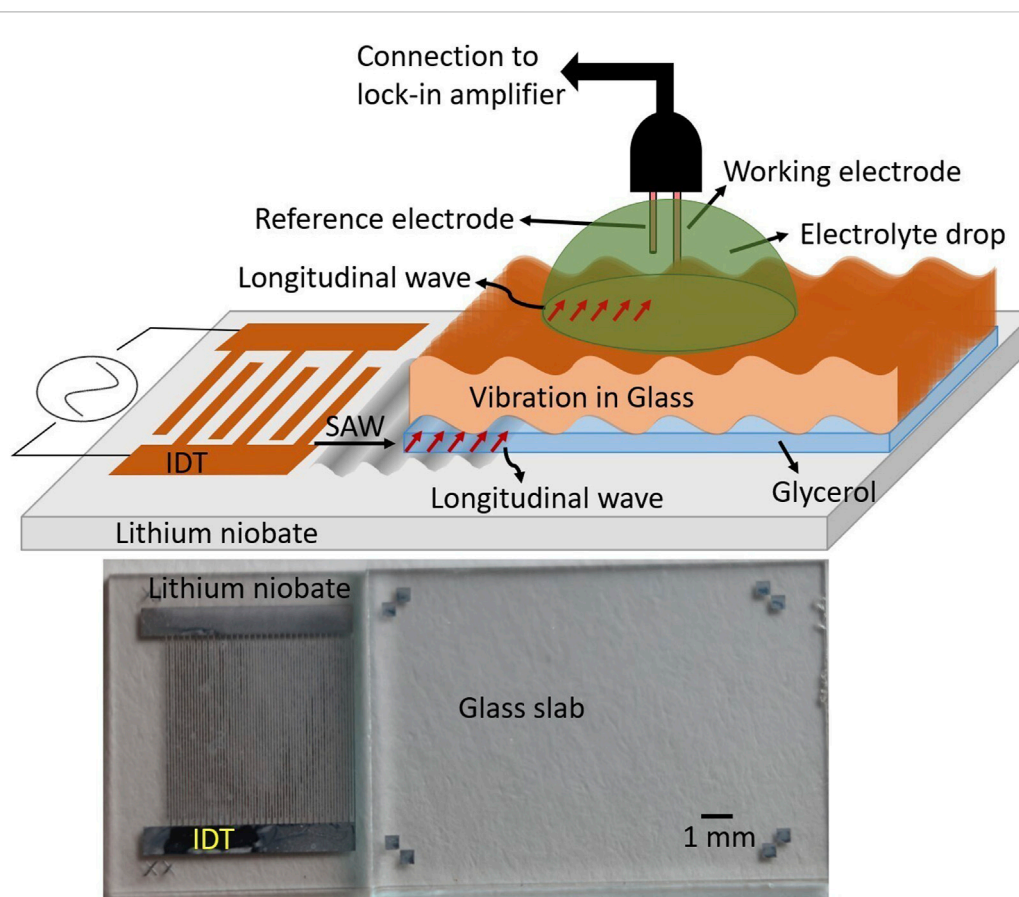


FIGURE 1

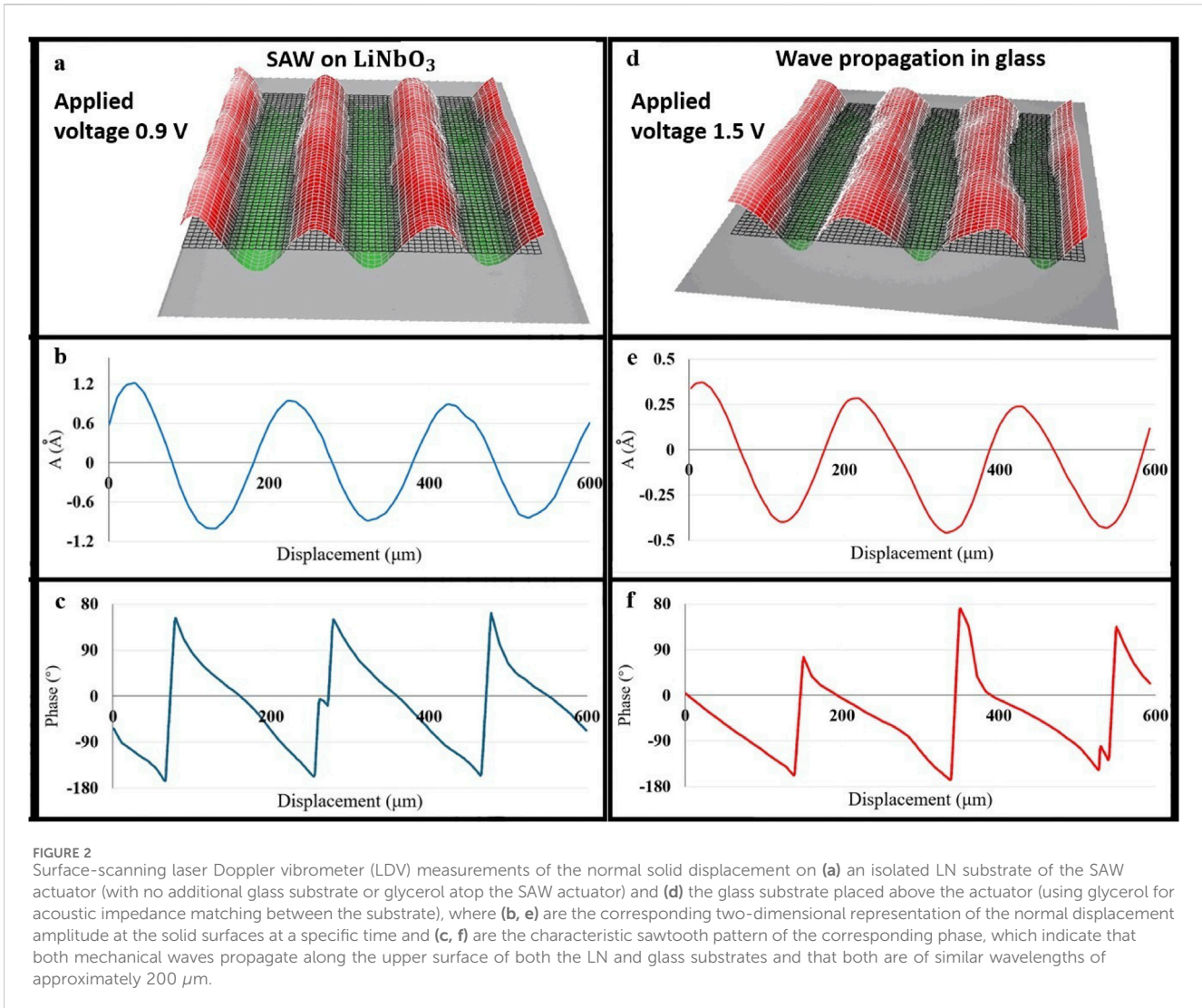
Sketch of the experimental setup and an image (below) of a 1-mm-thick glass slab atop an SAW actuator; interdigital transducer (IDT) comprising electrodes in contact with a piezoelectric substrate is shown to the left. We placed the glass slab atop the actuator, right of the IDT, using a thin layer of glycerol. We illustrate in the sketch the placement of a drop of electrolyte solution atop the glass slab, into which we inserted working and reference electrodes. The excited EDL leaks an electrical field that we measured using the working electrode.

signal counterpart. Previous theorems have predicted that the SAW mechanical component (Dubrovski and Manor, 2021) and the voltage signal in the piezoelectric substrate (Dietzel and Hardt, 2020) may both introduce electrokinetic effects in an electrolyte solution near the surface of the actuator. The former and the latter displace ions via the accompanying evanescent mechanical wave and the spreading of an electric field in the neighboring electrolyte solution, respectively. Moreover, the voltage signal counterpart of the SAW has been attributed to the electro-catalysis of chemical reactions by SAW actuators (Ahmed et al., 2019; Rezk et al., 2020). SAW actuators have also been used to measure the presence and dynamics of ions in neighboring electrolyte solutions (Aremanda and Manor, 2023). While the contribution of the voltage signal in the piezoelectric substrate of the actuator to electrokinetic effects in the neighboring electrolyte is trivial, it is not clear whether it dominates over contributions from the mechanical component of the SAW. To solve this question, we isolated the mechanical component of the SAW on a glass substrate neighboring an aqueous electrolyte solution. Our measurements confirmed significant electrokinetic effects in the electrical double layer (EDL), which spontaneously appears at the glass/electrolyte interface.

Electrical double layers are the opposing charge layers that spontaneously appear at the surface of a substrate in an

electrolyte. The majority of surfaces accumulate spontaneous charge when in contact with an electrolyte due to chemical or physical surface reactions. The charged surface attracts clouds of ions from the electrolyte, some of which will adsorb on the surface. Others, non-adsorbing ions, accumulate in nanometer-thick ion clouds near the charged surface, fully screening the electrical field emanating from the surface charge at equilibrium. EDLs are fundamental to countless natural and artificial systems. Examples of EDL electrokinetic applications include the electrophoretic particle motion, the electroosmotic actuation of flow (Hunter, 2001), and the electrowetting motion of liquid film and drops (Frieder and Jean-Christophe, 2005). Examples of equilibrium applications are energy barriers to particulate coagulation and adsorption (Chan et al., 2008; Homede et al., 2018, 2020), a guiding mechanism for folding structures of proteins (Zhou and Pang, 2018), and the origin of the surface electrical properties in biological (Hong and Okajima, 1986) and artificial membranes (Hoek and Tarabara, 2013).

Our analysis is reminiscent of the classic electroacoustic measurements of the interactions between bulk ultrasonic waves and ions in electrolyte solutions (Debye, 1933; Yeager et al., 1949; Dahint et al., 1992) or charged colloids in dispersions (Dukhin and



Goetz, 1996; Babchin et al., 1989; Hunter, 1998). These measurements have been employed to analyze ionic species in electrolytes and analyze the electrokinetic properties, most notably the zeta potential, of particle dispersions in electrolytes. In the latter case, the ultrasonic waves interact with the electrical double layers (EDLs) at the interface of particles and electrolytes along the ultrasonic path, which varies the electric potential across the dispersion.

However, the nanometer thickness of EDLs and their nano- to micro-second relaxation times pose a challenge to direct measurements of ion dynamics in an isolated and unique EDL. This challenge is circumvented by exciting an EDL at a flat interface using a MHz-level Rayleigh-type SAW. These are the same type of waves that occur in earthquakes when pressure and shear waves meet near the Earth’s outer crust, forming a large amplitude waves—Rayleigh waves (or equivalently Rayleigh SAWs) that travel—near the crust’s surface. Rayleigh waves travel near the surface of a substrate and support both normal and longitudinal particle motion. In the laboratory, SAWs are generated in the piezoelectric substrate of actuators, where they are accompanied by an electric signal counterpart. The mechanical component of the

SAW produces periodic boundary layer flows in the neighboring fluid—the equivalent of an evanescent mechanical wave—close to the surface of the solid (Rayleigh, 1884; Schlichting, 1932; Vanneste and Bühler, 2011; Manor et al., 2012). The leading-order period of the boundary layer flow is similar to the period (the inverse of frequency) of the SAW in the solid; its characteristic thickness—known as the viscous penetration of the SAW into the fluid—is 100 nm in ambient water neighboring a 20-MHz frequency SAW.

In the presence of an SAW in a solid substrate, the EDL at the solid/electrolyte interface is rendered out of equilibrium, leaking an electrical field to the electrolyte bulk. This electrical field leakage is proportional to the zeta potential of the solid surface in the electrolyte solution and is modulated in time by the motion of ions. Thus, the leakage obtains the frequency of the exciting SAW and its harmonics. Moreover, a SAW of MHz-level frequency, ω , comparable to the inverse of the ion relaxation times $D(i)/\sigma^2$, was found to introduce ion dynamic motion in the EDL, where $D(i)$ is the diffusion coefficient of ion i and $\sigma \equiv \sqrt{\epsilon k_B T / 2e^2 I}$ is the Debye length of the EDL, where I is the ionic strength of the electrolyte, and ϵ , k_B and T are the permittivity of the electrolyte solution,

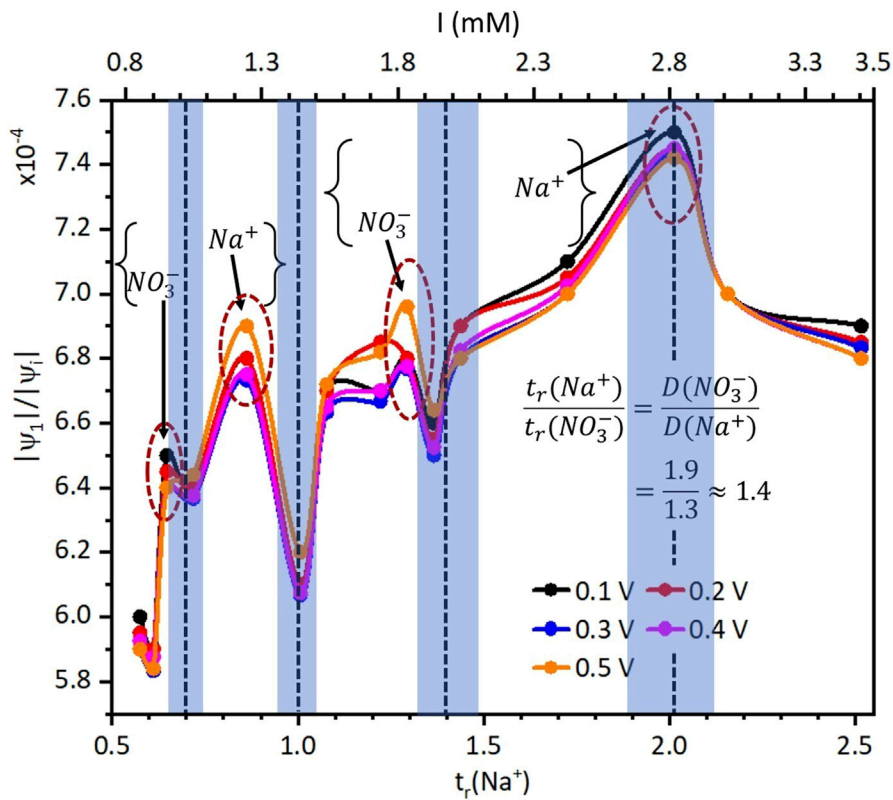


FIGURE 3 Ionic strength (I) and sodium ion based acoustic-to-EDL time-ratio ($t_r(Na^+)$) variations of the measured electrical field leakage (in terms of the electrical potential magnitude, $|\psi_i|$) for $NaNO_3$ solutions at different levels of the electrical potential applied to the actuator, $|\psi_1|$ (given in the legend in volts). We have circled in dashed red lines the measured electrical potential peaks that appear to correspond to ion relaxation times and their harmonics ($t_r(Na^+) \approx 1, 2$; $t_r(NO_3^-) \approx 1, 2$) and have placed dotted vertical lines to denote the corresponding theoretical relaxation times (the shaded areas indicate the uncertainty associated with the experimental uncertainty in the parameters used for the theoretical prediction). In agreement with [Aremanda and Manor \(2023\)](#), where the measurements were done directly on the SAW actuator, the measured voltage peaks for $NaNO_3$ are smaller than the theoretical values of the ion relaxation times. The lines connecting the measured points are visual guides.

Boltzmann constant, and temperature, respectively ([Dubrovski and Manor, 2021](#)).

The ratio of the acoustic period and the relaxation time of ion i in the EDL, $t_r(i) = D(i)/\sigma^2\omega = 2D(i)e^2I/\epsilon\kappa_B T\omega$, gives an indication of the proximity of the two characteristic times and is linearly proportional to the ratio between the electrolyte ionic strength and SAW frequency, I/ω . Measurements of the electrical field leakage from the excited EDL at the interface of a SAW actuator and various electrolyte solutions demonstrated that $t_r(i) \approx 1$ yields peaks in the measured electrical field. These peaks are specific to the mobilities of ions, giving an array of ion mobilities in the EDL. Synchronization between the period (the inverse of frequency) of the SAW and the ion relaxation time at $t_r(i) \approx 1$ enhances the periodic displacement of ions, which increases the magnitude of the electrical field leakage from the EDL. This leakage provides insights into static EDL properties such as zeta potential and ionic strength, in addition to capturing dynamic EDL behaviors such as ion relaxation times, which highlight the limiting time by which an isolated EDL may dynamically store and release charge ([Aremanda and Manor, 2023](#)).

However, when conducting the measurements directly on the piezoelectric substrate of the SAW actuator, it is unclear whether the

mechanical SAW or its electrical counterpart dominated the EDL excitation in the previous experiment. The periodic (AC) voltage (ψ_i) applied to the actuator governs both the SAW intensity and the level of its electrical potential counterpart in the piezoelectric substrate. The SAW generates the evanescent mechanical wave in the electrolyte, which vibrates ions in the EDL at the same frequency. The electrical potential counterpart generates a periodically varying electrical field in the electrolyte at the same frequency, migrating ions periodically, and generating ion vibration. Once the excitation ceases, the ions will diffuse back to form an equilibrium EDL. To isolate the contribution of the mechanical component of the SAW to the excitation of ions in the electrolyte, it is necessary to eliminate its electrical potential counterpart in the piezoelectric substrate of the SAW actuator.

Here, we isolated the contribution of the SAW—that is, of the mechanical vibration—to the leakage of the electrical field off the excited EDL by transferring the SAW from the actuator to a glass slab. The glass slab supports pure mechanical vibration, which excites ions in EDLs at the flat interface between the glass and a drop of electrolyte. We describe our experiment in [Section 2](#), show and discuss our results in [Section 3](#), and summarize and conclude our findings in [Section 4](#).

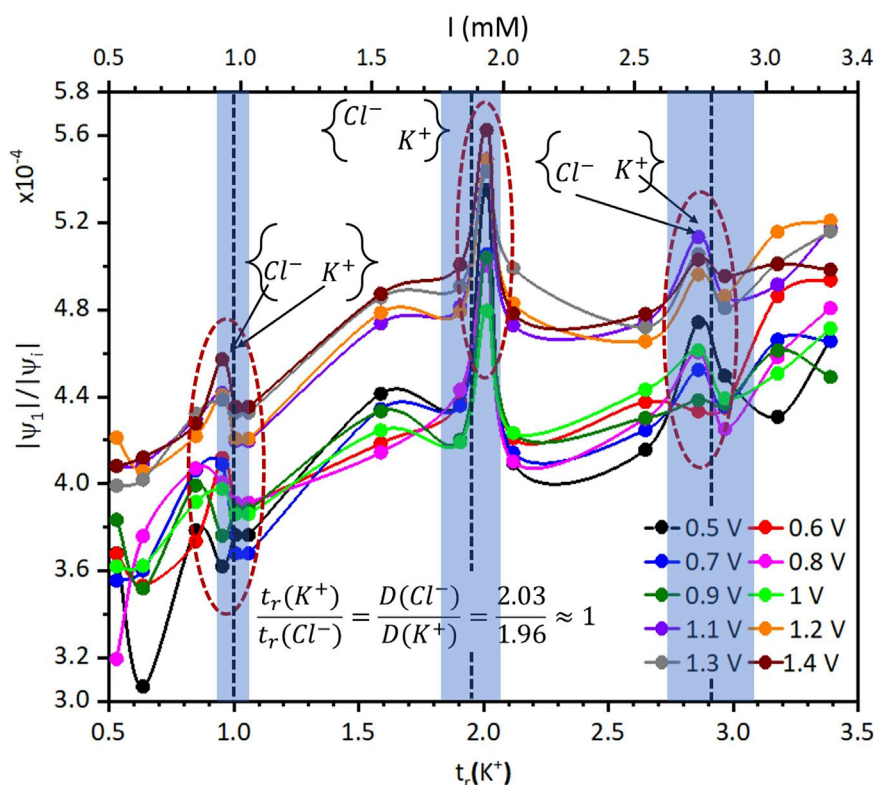


FIGURE 4

Ionic strength (I) and potassium ion based acoustic-to-EDL time-ratio ($t_r(K^+)$) variations of the measured electrical field leakage in terms of the electrical potential magnitude, $|\psi_1|/|\psi_i|$, for KCl solutions at different levels of the electrical potential applied to the actuator, $|\psi_a|$ (given in the legend in volts). We have circled in dashed red lines the measured electrical potential peaks that appear to correspond to ion relaxation times and their harmonics ($t_r(K^+) \approx t_r(Cl^-) \approx 1, 2, 3$) and have placed dotted vertical lines to denote the corresponding theoretical relaxation times (the shaded areas indicate the uncertainty associated with the experimental uncertainty in the parameters used for the theoretical prediction). In agreement with [Aremanda and Manor \(2023\)](#), where the measurements were done directly on the SAW actuator, the measured voltage peaks for KCl are similar to the theoretical values of the ion relaxation times. The lines connecting the measured points are visual guides.

2 Materials and methods

2.1 Experimental setup

The integrated ultrasonic device in [Figure 1](#) is comprised of a 1-mm-thick glass slab (microscope slides, 1 mm thick, tolerance: ± 0.05 mm, Marienfeld) which is attached to a flat piezoelectric lithium niobate (LN) substrate of a 20 MHz-frequency SAW actuator that supports a traveling SAW of $\lambda_{LN} = 200$ μm wavelength. We used glycerol (anhydrous, AR, Bio-lab Ltd.) as an ultrasonic impedance matching liquid film between the glass substrate and the actuator. The glycerol gap (film thickness) between the glass and LN substrates was approximately 40 μm . This value was set by dispensing a 5 μl drop of glycerol atop the LN substrate and then carefully placing the glass slab on top. The glycerol subsequently spread in the gap and filled the space due to capillary action. The capillary action further trapped the liquid within the gap. The glycerol volume and lateral dimensions of the spacing determine the gap thickness. Moreover, the glass surface became spontaneously charged at a level of -20 to -70 mV when in contact with an electrolyte and hence supported an EDL; see [Supplementary Information S1](#) for zeta potential measurements using an electrokinetic analyzer for solid surface analysis: SurPASS 3 (Anton Paar GmbH, Graz, Austria). Under similar conditions, the

piezoelectric LN substrate of the SAW actuator supports zeta potential levels in the range of -30 to -40 mV ([Aremanda and Manor, 2023](#)).

The SAW actuator is comprised of a 5-nm chrome/1,000 nm aluminum interdigital transducer (IDT) consisting of 30 electrode pairs of 50 μm width and gaps (between the electrodes) and an IDT aperture of 6 mm. The electrodes were patterned using standard photolithography on a 0.5-mm-thick 128° Y-cut, X-propagating single crystal lithium niobate, LiNbO₃, (LN) piezoelectric substrate (Roditi International, England) to support a traveling 20 MHz-frequency Rayleigh-type SAW. We used a signal generator (SMB100A, Rohde & Schwarz, Germany) to supply 20-MHz voltage signals to generate a SAW in the LN substrate. At the far end of the glass substrate from the IDT, we placed a 3-mm-wide strip of wet paper, which was found to be an efficient SAW absorber to eliminate wave reflections, although, as we will show, it was less effective in the glass substrate.

We dispensed a sessile drop of an electrolyte solution atop the glass substrate. The electrolyte solutions were prepared by dissolving ultrapure salts: NaNO₃ (sodium nitrate, ACS reagent, $\geq 99.0\%$, Sigma-Aldrich, Germany) and, separately, KCl (potassium chloride, ACS reagent, $\geq 99.0\%$, Variation Chemical MFG CORP, CA) in HPLC water. These are strong electrolytes that have small ion pairs and were chosen so that our EDLs were near ideal; they are well

described by the Boltzmann–Poisson equation at low ionic concentrations, so our experiments should follow the theory in [Dubrovski and Manor \(2021\)](#).

We then positioned the working and reference microelectrodes in the drop. The working electrode was positioned at a separation of 30–40 μm away from the glass substrate to avoid the anticipated dispersion of the electrical field leakage, ψ_1 , at separations greater than the 200 μm SAW-wavelength ([Dubrovski and Manor, 2021](#)). The electrodes were fixed to a stand, and the SAW actuator was placed on a vertical translation stage of 1 μm resolution and a 13 mm travel range (7VT40-13 Vertical Stage, Standa, Lithuania). The microelectrodes were made from a 30 AWG wire wrap with an inner conductor of a silver-plated copper wire of 0.25 mm diameter and an outer shrouding for insulation (KYNAR460, Pro-Power, Talmir electronics, Haifa, Israel). The reference electrode, which accounts for the electrical potential at the bulk of the drop, was placed at a separation of approximately 1 mm away from the solid.

The electrodes were connected through an active differential voltage probe (RT-ZD02, Rohde & Schwarz, Germany) to an RF lock-in amplifier (SR844, Stanford Research Systems, CA) for measuring the 20 MHz-frequency component of the electrical leakage—the linear (same frequency) response of the EDL to the exciting SAW. We used a BNC T-connector (50 Ω , Cinch Connectivity Solutions, Talmir electronics, Haifa, Israel) to split the signal sent to the actuator so that we simultaneously supplied the same signal to the lock-in amplifier's reference-signal port.

2.2 Transport of the mechanical field through the integrated device

The SAW in an isolated actuator (no glass substrate or glycerol layer) is a propagating Rayleigh wave in the presence of the wave absorber at the edge of the actuator ([Figure 2a-c](#)). In the integrated SAW actuator/glycerol/glass device, the SAW in the actuator translates to a same-frequency mechanical vibration in the glass substrate through the glycerol matching layer via diffraction ([Figure 2d,e,f](#)). We observed a propagating mechanical vibration at the glass surface close to the IDT—that is, close to the electrodes on the SAW actuator.

To realize the transport of mechanical power from the SAW actuator to the glass substrate, we measured the normal vibration at the LN upper surface of the SAW actuator (at the LN/glycerol interface) and at the glass upper surface (at the glass/air interface) of the integrated SAW actuator/glycerol/glass device at separations of 1, 5, 8, and 12 mm from the IDT—see the measurement results in [Supplementary Information S3](#), where we give the corresponding autocorrelation coefficient to compare the two vibration modes on the two substrates that comprise the integrated device. The vibration normal amplitude is similar on both the LN and glass substrate, and both support a similar wavelength of approximately 200 μm . However, while both vibrations at the LN and glass substrates are nearly a propagating wave at separations of 1 and 5 mm from the IDT, at separations of 8 and 12 mm, the vibration becomes a clear combination of propagating and standing waves. The appearance of a nearly propagating wave on both substrates near the IDT and a combination of a propagating and standing wave far from the IDT is likely a result of asymmetry. The vibration source

(IDT at the SAW actuator) is fabricated on one side of the integrated device; the vibration is reflected from the opposite side of the device while undergoing attenuation by the glycerol film and by the wave absorber placed on the glass substrate at the far edge of the integrated device from the IDT.

In the absence of a sessile drop of an electrolyte solution, the phase of the mechanical vibration through the integrated device changed with separation from the IDT at the SAW actuator. Moreover, the vibration in the LN and glass substrates appeared synchronized. At separations from the IDT, where the SAW in the actuator is nearly a propagating wave or a combination of a propagating and standing wave, so was the mechanical vibration in the glass substrate directly above. Moreover, the SAW in the actuator did not attenuate by simple diffraction to the glass substrate. Such a simple diffraction would be the case if the glass substrate above the SAW actuator were a half-space of glass. In this case, we would expect the SAW in the actuator to almost fully attenuate at a separation of 1 mm from the point where it propagated under the glycerol film and glass substrate (see [Supplementary Information S2](#) for details). However, our measurements suggest that the vibrations in the LN and glass substrate in the integrated device are intimately connected, suggesting that power is transferred from the SAW actuator to the glass substrate and from the glass substrate back to the LN substrate. This behavior may suggest that the mechanical vibration in the glass substrate is akin to a Lamb wave, in which the mechanical vibration is spread throughout the substrate, continuously absorbing and reflecting power to and from the SAW actuator, respectively.

Moreover, in the presence of a sessile drop of an electrolyte solution (as in our experiment) atop the glass substrate of the integrated device, the sessile drop absorbs some of the mechanical power in the glass, and hence one should expect that less mechanical power reaches the far end of the integrated device and, hence, a reduced wave reflection off the glass edge far from the IDT. That is, one should expect a more pronounced propagating mechanical wave in the glass substrate. However, measuring the vibration under the drop is a challenge due to its curved free surface and is beyond the scope of the current investigation.

We are predominantly interested in the mechanical vibration at the upper surface of the glass. It is interesting that it is of similar frequency and wavelength to the SAW in the actuator, which determine the frequency of ion excitation in the EDL at the glass/electrolyte interface and the separation between the working electrode and the glass surface that will facilitate the measurement of the electrical field leakage off the EDL, respectively. Our investigation indicates that the similarity between the frequency and wavelength of the vibration in glass and LN should result in a similar (although not the same) mechanical excitation of the ions in our experiment to that previously generated by a direct contact between the electrolyte and the LN substrate of the SAW actuator.

2.3 Transport of the electrical field through the integrated device

The electrical field accompanying the mechanical wave in the piezoelectric LN substrate of the actuator also spread into the glass substrate through the separating glycerol layer. In the absence of

charges in the amorphous glass, the electrical potential ψ is governed by the Poisson equation,

$$\nabla^2 \psi = 0. \tag{1}$$

The spatiotemporal distribution of the electrical potential in the glass is solved subject to the electrical potential signal accompanying the mechanical wave at the solid surface of the LN substrate at $y = 0$, which is approximately given by the real component of

$$\psi(y = 0) = \text{real}(|\psi_i|e^{i(\omega t - \kappa_x x)}), \tag{2}$$

where $|\psi_i|$ is the amplitude of the electrical potential input to the piezoelectric substrate of the SAW actuator in our experiment, $\omega = 2\pi \times 20$ MHz is the SAW angular frequency, $\kappa_x = 2\pi/\lambda_{\text{LN}} - i\alpha$ is the complex SAW wavenumber, and x is a coordinate along the LN surface, commencing where the LN surface is first in contact with glass along the path of the SAW. We further assume the decay of ψ in a half-space of glass,

$$\psi(y \rightarrow \infty) = 0. \tag{3}$$

The problem in Equations 1–3 is satisfied by the electrical potential in a half-space of glass,

$$\begin{aligned} \psi &= \text{real}(|\psi_i|e^{i(\omega t - \kappa_x x - \kappa_y y)}) \\ &= |\psi_i| \cos\left(\omega t - \frac{2\pi}{\lambda_{\text{LN}}}x + \alpha y\right) \times e^{(-\alpha x - \frac{2\pi}{\lambda_{\text{LN}}}y)} \end{aligned} \tag{4}$$

where $\kappa_y = -i\kappa_x$. The exponential attenuation of the electrical field suggests that the magnitude of the spatiotemporal harmonic electrical potential generated by the actuator vanishes in the glass substrate. In our case, where the SAW does not appear to attenuate in the LN substrate of the actuator, we can approximate that the attenuation coefficient vanishes ($\alpha \approx 0$), and hence the electrical potential amplitude at the upper surface of the glass substrate (given at $y = 1$ mm) is

$$\begin{aligned} |\psi| &\approx |\psi_i|e^{-(\alpha x + \frac{2\pi}{\lambda_{\text{LN}}}y)} \approx |\psi_i|e^{-(\frac{2\pi}{0.2\text{mm}} \times 1\text{mm})} \\ &\approx |\psi_i|e^{-31} = |\psi_i|e^{-31} \approx 3 \times 10^{-14}|\psi_i|. \end{aligned} \tag{5}$$

The electrical field accompanying the mechanical vibration in the actuator decays in the glass substrate, reaching a negligible magnitude at the upper surface of the glass. We will show later that the electrical potential measured is three to four orders of magnitude smaller than $|\psi_i|$. Hence, it is the mechanical wave alone that reaches the upper surface of the glass to excite the EDL at the glass/electrolyte interface.

3 Results and discussion

In Figures 3, 4 we show the ionic strength variations of the measured electrical field leakage in terms of a voltage spectrum, which we obtained for different magnitudes of the applied voltage to the SAW actuator ($\psi_i = |\psi_i| \cos(\omega t)$) in two electrolyte solutions: sodium nitrate (NaNO_3) and potassium chloride (KCl). We scaled the magnitude of the measured voltage $|\psi_1|$ by the magnitude of the applied voltage to the SAW actuator $|\psi_i|$. The scaling was previously shown to collapse the data on a common curve when the measurement was conducted directly on the SAW actuator. These previous

measurements exposed the EDL to both the mechanical SAW and the electrical counterpart signal in the piezoelectric LN substrate of the SAW actuator (Aremanda and Manor, 2023). Moreover, we added to the figures an additional horizontal axis that quantifies the ratio between the acoustic time period and the positive ion relaxation time through the EDL—that is, $t_r(\text{Na}^+) = D(\text{Na}^+)/\sigma^2\omega$ in Figure 3 and $t_r(\text{K}^+) = D(\text{K}^+)/\sigma^2\omega$ in Figure 4.

In our current experiments, we eliminated the electrical signal in the SAW actuator by transferring the mechanical component of the SAW to a mechanical vibration in the neighboring glass substrate. The intensity of the SAW in the actuator was linearly proportional to $|\psi_i|$ (Royer et al., 1999) in the low applied voltage levels used in our experiments, where $|\psi_i| = 0.1 - 1.5$ V. Since the transport of the ultrasonic wave is a linear process (Morse and Ingard, 1986), the amplitude of the vibration in the glass, which is generated by the SAW, is linear with $|\psi_i|$ as well. Hence, scaling $|\psi_1|$ by $|\psi_i|$ on glass is proportional to scaling $|\psi_1|$ by the unattenuated displacement amplitude of the mechanical vibration at the glass surface.

The choice of electrolyte solutions is such that one (NaNO_3) possesses dissociated ions of dissimilar diffusion coefficients, while the other (KCl) has ions with similar diffusion coefficients. The diffusion coefficients of the positive ($D(\text{Na}^+)$) and negative ($D(\text{NO}_3^-)$) ions in the sodium nitrate solutions used are 1.33×10^6 m²/s and 1.90×10^6 m²/s, respectively. Likewise, the diffusion coefficients of the positive ($D(\text{K}^+)$) and negative ($D(\text{Cl}^-)$) ions in the potassium chloride solutions used are 1.96×10^6 m²/s and 2.03×10^6 m²/s, respectively. However, the resolution of our measurement, which is sensitive to a precision of two significant digits in the diffusion coefficients, renders the contribution of the diffusion coefficients to the voltage leakage in the case of KCl the same. At a precision of two significant digits, the corresponding diffusion coefficients are $D(\text{K}^+) \approx D(\text{Cl}^-) \approx 2.0 \times 10^6$ m²/s.

The electrical field leakage measured as an electrical potential spectra is the response of the EDL to the MHz-level mechanical vibration in glass that is in contact with NaNO_3 and KCl solutions and originates from the zeta potential of the EDL; the measurements follow Dubrovski and Manor (2021). In the case of NaNO_3 , we observed peaks in the magnitude of the measured electrical potential where the vibration temporal period (inverse of SAW frequency) was similar to the ion relaxation time near $t_r(\text{Na}^+) = 1, 2$ and $t_r(\text{NO}_3^-) = 1, 2$. In Figure 3, we used $t_r(\text{Na}^+)$ for the horizontal axis so that $t_r(\text{NO}_3^-) = (D(\text{Na}^+)/D(\text{NO}_3^-)) \times t_r(\text{Na}^+) = 1, 2$ translates to $t_r(\text{Na}^+) = 1 \times (D(\text{Na}^+)/D(\text{NO}_3^-))$, $2 \times (D(\text{Na}^+)/D(\text{NO}_3^-)) \approx 0.7, 1.4$, which is the horizontal axis position of the peaks for NO_3^- . In the case of KCl in Figure 4, both ions possess similar diffusion coefficients so that $t_r(\text{K}^+) \approx t_r(\text{Cl}^-)$, and thus we observe the same peaks at $t_r(\text{K}^+) \approx 1, 2, 3$ for both ions.

The excitation of the EDL at the glass–electrolyte interface in our measurement was solely mechanical. It is useful to compare our results to Aremanda and Manor (2023), where the excitation of the EDL at the SAW actuator/electrolyte interface comprised both a mechanical vibration component (Rayleigh SAW) and its electrical potential counterpart in the piezoelectric LN substrate of the actuator. We observed three points of comparison. (a) We measured peaks of the voltage leakage, $|\psi_1|$, where the periodic time of the vibration was found to be similar to the relaxation time of ions in both studies. (b) The measured magnitude of $|\psi_1|$ was similar in both studies. (c) Scaling $|\psi_1|$ by the applied voltage to the SAW

actuator, $|\psi_i|$, collapsed the measured results onto unifying curves in both cases, although, in Figure 4, we observe two unifying curves associated with lower and higher levels of $|\psi_i|$.

The first point of comparison—the measured $|\psi_1|$ peaks when exciting EDLs on glass or directly on the piezoelectric substrate of the SAW actuator (Aremanda and Manor, 2023)—highlighted that the solid vibration alone is sufficient to generate the electrokinetic motion of ions in the excited EDL. Moreover, the solid vibration-supported peaks in the electrical field leakage from the EDL appeared when the vibration period was similar to the relaxation time of a specific ion in the EDL.

Moreover, the measured voltage peaks to originate from the NaNO_3 electrolyte appeared in the previous measurement and the present study similarly at acoustic to ion relaxation time ratios that are smaller by approximately 15% relatively to the theoretical values for both Na^+ and NO_3^- ions. In both cases, their harmonics appeared to be closer to the corresponding theoretical values. However, in the case of the KCl electrolyte, we obtained measured voltage peaks that agree well with the theoretical values for the acoustic to ion relaxation time ratios, $t_r(K^+) \approx t_r(\text{Cl}^-) = 1, 2, 3$.

A second point of comparison was the similar magnitude of the measured voltage, $|\psi_1|$, when exciting EDLs on glass or directly on the piezoelectric substrate of the SAW actuator. This finding suggests that exciting ions in EDLs on glass using a mechanical vibration introduces a similar order contribution to $|\psi_1|$ compared to exciting EDLs directly on the SAW actuator, where the mechanical vibration is convoluted with an electrical signal in the piezoelectric substrate of the actuator. This became evident when comparing our results measured on glass to those of the previous study, where the measurement was directly on the substrate of the SAW actuator. Although in both cases the measurements were of similar order of magnitude, the measured to applied (to the actuator) voltage ratio, $|\psi_1|/|\psi_i|$, was greater in the previous study by a factor of approximately two to three when compared to the current study. This difference could be attributed to a lower mechanical vibration displacement on the glass upper surface of the integrated device compared to the vibration displacement magnitude on an isolated SAW actuator per the applied voltage level, $|\psi_1|$ (it should be noted that similar SAW actuators, fabricated in the same photolithography process, were used in the two different studies).

The third point was about the scaling of the measured voltage, $|\psi_1|$, by the applied voltage magnitude to the piezoelectric actuator, $|\psi_i|$. The scaling collapsed the measured data in our measurements on glass to one unifying curve in the case of the NaNO_3 solution and to two unifying curves in the case of the KCl solution, one for the lower $|\psi_i|$ regime and another (associated with a greater $|\psi_1|/|\psi_i|$ response magnitude by approximately 15%–20%) for the greater $|\psi_i|$ regime. The collapse of the measured data to unifying curves by the scaling $|\psi_1|/|\psi_i|$ was observed to be similar to the collapse of data in the previous measurements on the piezoelectric substrate of the SAW actuator (Aremanda and Manor, 2023). Dubrovski and Manor (2021) suggested that $|\psi_1|$ scales similarly with the zeta potential of the EDL and with the unattenuated magnitude of the mechanical vibration at the surface from which the EDL emanates into the electrolyte in both the current and previous measurements. Hence, the similar collapse of the data by using $|\psi_i|$ to scale the measured voltage signal $|\psi_1|$ and the similar order of magnitude of the ratio $|\psi_1|/|\psi_i|$ suggest similar governing physical mechanisms in both the

current and previous measurements, albeit the collapse of our current KCl data to two unifying curves is a caveat to this understanding that should be investigated in further research. Overall, the similarity between the collapse of the measured data in the current measurement on glass and in the previous measurement on LN strengthens the theoretical prediction that $|\psi_1|$ is predominantly generated by the mechanical solid vibration.

4 Conclusion

A previous direct measurement of the dynamic electrokinetic properties of an isolated and unique EDL system (Aremanda and Manor, 2023) overcame the challenges in observing the dynamics of ions therein by using MHz-level SAWs, which render the EDL out of equilibrium and cause the leakage of electrical fields. The electrical field leakage baseline is connected to the EDL zeta potential and is modulated by the ion mechanical vibration. The leakage undergoes local maxima levels, where the exciting SAW temporal period synchronizes with the ion relaxation time in the EDL. However, the EDL was measured at the interface between the electrolyte and the piezoelectric LN substrate of the SAW actuator, which supports both a Rayleigh-type SAW—a mechanical vibration—and a voltage signal counterpart. The relative contributions of the two mechanisms to the EDL excitation were not investigated, although Dubrovski and Manor (2021) hinted at a greater contribution from the SAW.

Here, we answered this question by isolating the mechanical vibration in glass. The glass substrate—a dielectric—attenuated the electrical field counterpart of the SAW in the actuator piezoelectric substrate due to the SAW finite wavelength. The thickness of the glass substrate was five times the SAW wavelength, and hence attenuated the electrical field emanating from the actuator to a level many orders of magnitude smaller than the measured electrical field leakage off the EDL at the glass/electrolyte interface. We studied similar electrolyte systems to those measured previously atop the SAW actuator, using ion mixtures of different and similar diffusion coefficients; the ion diffusion coefficient alongside the EDL Debye length determined the corresponding EDL relaxation time. We thus showed that the mechanical vibration alone is sufficient to introduce measurable electrokinetic effects in an EDL, that this component introduces at least the same magnitude of electrical field leakage off the EDL, and that the scaling that collapses the measured electrical field (voltage) curves, $|\psi_1|$, at different SAW intensity levels onto a unifying curve is the same for EDLs on glass and the SAW actuator.

The difference between classic electroacoustic studies and this one is that in classic electroacoustics, bulk ultrasonic waves generate an electrical potential difference across a volume of electrolyte solution or a colloidal suspension in electrolyte. Here, we excited ions in an isolated EDL emanating from a flat solid surface in contact with electrolytes by generating an ultrasonic vibration in the solid. Our work shows that future studies in this field may measure the static and dynamic electrokinetic properties of flat solid surfaces, provided that the solid substrate supports a corresponding mechanical vibration. For example, silica-based glass substrates, such as the one in our experiment, are widely used for surface chemistry manipulation, and hence is a versatile platform to study the dynamic motion of ions in EDLs generated by different surface

chemistries in contact with an electrolyte, which may be used, for example, for membranes, batteries, and supercapacitors.

Moreover, we highlighted that a mechanical vibration traveling along a solid substrate in an electrolyte solution introduces electrokinetic effects. Ions vibrate in the EDL at the frequency of the mechanical vibration. Thus, out-of-equilibrium EDLs must be accounted for, especially in micro- and nano-fluidic systems that are actuated by mechanical vibration, such as SAWs. For example, on such platforms, EDLs that govern ion transport through ion-sensitive membranes or govern the stability of liquid films may not be at equilibrium and hence may possess different electrical properties from equilibrium EDLs; out-of-equilibrium EDLs may alter the membrane ion screening properties and the stability of the liquid films.

Data availability statement

The original contributions presented in the study are included in the article/[Supplementary Material](#); further inquiries can be directed to the corresponding author.

Author contributions

SA: formal analysis, investigation, methodology, validation, writing – original draft, and writing – review and editing. YL: investigation and writing – review and editing. GO: investigation, validation, and writing – review and editing. OM: conceptualization, formal analysis, funding acquisition, methodology, project administration, supervision, and writing – original draft.

Funding

The author(s) declare that financial support was received for the research and/or publication of this article. This research was

supported by the Ministry of Innovation, Science & Technology of the State of Israel, grant number 1001827275, and by the Israel Science Foundation, grant number 520/24.

Conflict of interest

The authors declare that the research was conducted in the absence of any commercial or financial relationships that could be construed as a potential conflict of interest.

The author(s) declared that they were an editorial board member of *Frontiers* at the time of submission. This had no impact on the peer review process and the final decision.

Generative AI statement

The authors declare that no generative AI was used in the creation of this manuscript.

Publisher's note

All claims expressed in this article are solely those of the authors and do not necessarily represent those of their affiliated organizations, or those of the publisher, the editors and the reviewers. Any product that may be evaluated in this article, or claim that may be made by its manufacturer, is not guaranteed or endorsed by the publisher.

Supplementary material

The Supplementary Material for this article can be found online at: <https://www.frontiersin.org/articles/10.3389/facou.2025.1568083/full#supplementary-material>

References

- Ahmed, H., Rezk, A. R., Richardson, J. J., Macreadie, L. K., Babarao, R., Mayes, E. L. H., et al. (2019). Acoustomicrofluidic assembly of oriented and simultaneously activated metal-organic frameworks. *Nat. Commun.* 10, 2282. doi:10.1038/s41467-019-10173-5
- Aremanda, S., and Manor, O. (2023). Measurements of ion dynamics and electro-mechanical resonance in an electrical double layer near a surface acoustic wave. *J. Phys. Chem. C* 127, 20911–20918. doi:10.1021/acs.jpcc.3c05063
- Babchin, A., Chow, R., and Sawatzky, R. (1989). Electrokinetic measurements by electroacoustical methods. *Adv. Colloid Interface Sci.* 30, 111–151. doi:10.1016/0001-8686(89)80005-3
- Chan, D. Y., Manor, O., Connor, J. N., and Horn, R. G. (2008). Soft matter: from shapes to forces on the nanoscale. *Soft Matter* 4, 471–474. doi:10.1039/b712924f
- Dahint, R., Grunze, M., Josse, F., and Andle, J. (1992). Probing of strong and weak electrolytes with acoustic wave fields. *Sensors Actuators B Chem.* 9, 155–162. doi:10.1016/0925-4005(92)80209-G
- Debye, P. (1933). A method for the determination of the mass of electrolytic ions. *J. Chem. Phys.* 1, 13–16. doi:10.1063/1.1749213
- Dietzel, M., and Hardt, S. (2020). Electroosmotic flow in small-scale channels induced by surface-acoustic waves. *Phys. Rev. Fluids* 5, 123702. doi:10.1103/physrevfluids.5.123702
- Dubrovski, O., and Manor, O. (2021). Revisiting the electroacoustic phenomenon in the presence of surface acoustic waves. *Langmuir* 37, 14679–14687. doi:10.1021/acs.langmuir.1c02414
- Dukhin, A. S., and Goetz, P. J. (1996). Acoustic and electroacoustic spectroscopy. *Spectroscopy* 12, 4336–4344. doi:10.1021/la951086q
- Frieder, M., and Jean-Christophe, B. (2005). Electrowetting: from basics to applications. *J. Phys.* 17, R705–R774. doi:10.1088/0953-8984/17/28/r01
- Gu, Y., and Li, D. (2000). The zeta-potential of glass surface in contact with aqueous solutions. *J. Colloid Interface Sci.* 226, 328–339. doi:10.1006/jcis.2000.6827
- Hoek, E. M. V., and Tarabara, V. V. (2013). *Encyclopedia of membrane science and technology*. Hoboken, NJ: Wiley Online Library.
- Homede, E., Abo Jabal, M., and Manor, O. (2020). Connecting surface-forces-based energy barriers to nonhomogeneous colloidal structures to appear from volatile binary mixtures of same size nanoparticle species. *Adv. Func. Mater.* 30, 2005486. doi:10.1002/adfm.202005486
- Homede, E., Zigelman, A., Abezgauz, L., and Manor, O. (2018). Signatures of van der Waals and Electrostatic Forces in the Deposition of Nanoparticle Assemblies. *Phys. Chem. Lett.* 9, 5226–5232. doi:10.1021/acs.jpcclett.8b02052
- Hong, F. T., and Okajima, T. L. (1986). *Electrical double layers in pigment-containing biomembranes*. Boston, MA: Springer US, 129–147. doi:10.1007/978-1-4684-8145-7_10
- Hunter, R. J. (1998). Review Recent developments in the electroacoustic characterisation of colloidal suspensions and emulsions, 30.
- Hunter, R. J. (2001). *Foundations of colloid science/Robert J. Hunter*. 2nd Edn. Oxford University Press, 375–378.

- Manor, O., Yeo, L. Y., and Friend, J. R. (2012). The appearance of boundary layers and drift flows due to high-frequency surface waves. *J. Fluid Mech.* 707, 482–495. doi:10.1017/jfm.2012.293
- Morse, P., and Ingard, K. (1986). “Theoretical acoustics,” in *International series in pure and applied physics*. Princeton University Press.
- Rayleigh, L. (1884). On the circulation of air observed in Kundt’s tubes, and on some allied acoustical problem. *Phil. Trans. Roy. Soc.* 175, 1–21.
- Rezk, A. R., Ahmed, H., Brain, T. L., Castro, J. O., Tan, M. K., Langley, J., et al. (2020). Free radical generation from high-frequency electromechanical dissociation of pure water. *Phys. Chem. Lett.* 11, 4655–4661. doi:10.1021/acs.jpcclett.0c01227
- Royer, D., Lyle, S., and Dieulesaint, E. (1999). “Elastic waves in solids II: generation, acousto-optic interaction, applications,” in *Advanced texts in physics*. Berlin Heidelberg: Springer.
- Salzmann, E., and Dransfeld, K. (1967). Elastic surface waves in quartz at 316 MHz. *Appl. Phys. Lett.* 10, 3.
- Schlichting, H. (1932). Calculation of even periodic barrier currents. *Phys. Z.* 33, 327–335.
- Vanneste, J., and Bühler, O. (2011). Streaming by leaky surface acoustic waves. *Proc. R. Soc. A* 467, 1779–1800. doi:10.1098/rspa.2010.0457
- Yeager, E., Bugosh, J., Hovorka, F., and McCarthy, J. (1949). The application of ultrasonic waves to the study of electrolytic solutions II. The detection of the Debye effect. *J. Chem. Phys.* 17, 411–415. doi:10.1063/1.1747269
- Zhou, H.-X., and Pang, X. (2018). Electrostatic interactions in protein structure, folding, binding, and condensation. *Chem. Rev.* 118, 1691–1741. doi:10.1021/acs.chemrev.7b00305